Preferred citation: N. Postulka, M. Seibert, A. Geißler, M. Fricke, D. Bothe, T. Meckel and M. Biesalski. Porosity centrifuge: analysis of the porous structure of paper in contact with water under hypergravity conditions. In *Advances in Pulp and Paper Research*, Cambridge 2022, Trans. of the XVIIth Fund. Res. Symp. Cambridge, 2022 (D. Coffin and W. Batchelor, eds), pp 463–482. FRC, Manchester, 2022. DOI: 10.15376/frc.2022.1.463.

POROSITY CENTRIFUGE: ANALYSIS OF THE POROUS STRUCTURE OF PAPER IN CONTACT WITH WATER UNDER HYPERGRAVITY CONDITIONS

Niels Postulka[1], Michelle Seibert[1], Andreas Geißler[1], Mathis Fricke[2], Dieter Bothe[2], Tobias Meckel[1] and Markus Biesalski[1,]*

[1] Macromolecular Chemistry and Paper Chemistry, Department of Chemistry, Technical University of Darmstadt, Alarich-Weiss-Str. 8, 64287 Darmstadt, Germany

[2] Mathematical Modelling and Analysis, Department of Mathematics, Technical University of Darmstadt, Alarich-Weiss-Str. 10, 64287 Darmstadt, Germany

ABSTRACT

The characterization of pore sizes in paper is an important parameter, as numerous modifications of paper fibers influence or even aim to change them. Yet, most methods for determining pore size only work in the absence of water (e.g. mercury porosimetry or computed tomography). However, the influence of swelling on pore size caused by water is of great interest, especially, but not only, for the porous material paper.

Here we present a new method for determining the characteristic pore radius of paper sheets, being in direct contact with water. We call our device “porosity centrifuge”, in which the capillary forces that develop during the wetting and swelling process within a paper sheet are counter-balanced by a matching centrifugal force. While the

* Corresponding author

capillary pressure is determined by the pore radius of the porous structure, some paper intrinsic parameters lead to a reduction from the predicted imbibition distance calculated from the force balance between centrifugal and capillary forces. Since we are able to modulate the degree of this reduction by changing the fiber type or by applying various fiber pretreatments, such as beating, reduction of fines content or calendering, we refer to it as "substrate coefficient". Our method enables a simple and fast determination of characteristic pore radii in paper sheets using water as liquid.

1. INTRODUCTION

The characterization of pores in paper material is usually performed by Hg-porosity or solute exclusion tests to gain information about the pore size distribution. [1, 2] Only much smaller pores in the low nanometer range are usually analyzed through physisorption of gas molecules (BET technology). [3] These methods provide reliable information about the various pore radius distributions, which gives a good approximation to evaluate the capillary-based driving pressure for a wetting fluid. However, none of these methods take into account the counter force that occurs during the measurements. However, the physical description of the latter is, in contrast to capillary force, very complex. It is influenced by various intrinsic parameters such as tortuosity, surface morphology, surface porosity, swelling and fiber stiffness and also by extrinsic parameters such as surface boundaries, temperature and geometry. [4–8] Conclusions about the impact of this force can be drawn through velocity measurements during dynamic experiments. Several attempts have been made to mathematically describe the capillary-driven flow behavior, but especially for paper-based materials this is still a challenge, due to the numerous material-specific variables. [9] The equation most commonly used in this context was developed already in 1921 and is known as the "Lucas-Washburn equation": [10]

$$s(t) = \sqrt{\frac{\gamma D \cos(\theta)}{4\eta} t} \tag{1}$$

This formula impresses by its simplicity, since it assumes that the driving capillary pressure is balanced by the pressure drop, which Hagen-Poiseuille postulated for laminar flows in pipes assuming constant surface tension (γ) and viscosity (η), respectively. However, wetting and swelling induced changes of parameters like e.g. the dynamic contact angle (θ) or pore diameter (D), remain unconsidered. [11, 12, 13]

As has been shown by a large number of studies, the wetting distance of the fluid within a paper-based material linearly increases with the square root of time, as suggested by the Lucas-Washburn equation (1). [14] In particular, it has been reported that a calculation of the characteristic pore radius using experimental liquid transport data in paper results in pore size data that is up to 25 times lower than values determined via Hg porosity. [8] The difference is discussed to be caused by an inaccurate description of the fluid dynamics in paper, when disregarding paper intrinsic (fiber fibrillation, fiber surface porosity, fiber swelling etc.) as well as extrinsic parameters (rel. humidity/temperature dissolved fines from the fibers etc.). [13]

Note that some intrinsic parameters like fibrillation and fiber surface porosity may not affect the pore radius and thus impact capillary pressure, but have a strong impact on the pressure drop and thus on fluid dynamics. On the other hand, a shift of the characteristic pore radius, for example by paper compression, according to Hagen Poiseuille, also influences the pressure drop. Therefore, there is an inversely proportional relationship between the two factors. [15]

Our group recently introduced what we call a "porosity centrifuge" [16] to evaluate the characteristic pore radius of paper-based material in the solvent (water) wetted state. In principle, the base of this analytical technique has some similarities to well-known lab-on-disc devices. In brief, a narrow strip of paper is fixed on a rotating chuck and the imbibition of fluid into this strip is counteracted by generating a centrifugal force. Once the forces become equal, fluid propagation comes to a halt. This initial study focused on the introduction of the method and showed that dynamic processes such as fluid transport in paper can be investigated under quasi-stationary conditions. Here we systematically examine many different paper samples to show that the method also works quite well for routine investigations of lab-manufactured papers that differ in their intrinsic and extrinsic parameters, in order to learn how these determine the pore radii. In addition to parameters that can be influenced before and during the paper making process, like e.g. grammage, fractionation and milling degree of the fibers, modifications of the final paper were also investigated. Among these were the influence of paper compression and the width of hydrophilic channels produced via wax printing and subsequent melting. The result of these investigations suggest that the porosity centrifuge can be used to perform in-depth studies of paper interacting with fluids to learn more about the fascinating structure-property relation of paper in a solvent swollen state.

2. MATERIALS AND METHODS

2.1. Manufacturing Lab-engineered Paper

Lab engineered papers were generated by a Rapid-Koethen method in order to create equal tortuosity properties with isotropically layered fibers, according to

DIN 54358 and ISO 5269/2 in absence of any fillers and additives. Differently bleached pulps of Eucalyptus-, Northern Bleached Softwood Kraft- (NBSK-) and cotton linters pulps were used. With the exception of the latter, all pulps were prepared at different freeness levels, using energies of 0, 15, 50, 100, 150 and 200 kWh/t. Linters pulp was solely beaten with a constant energy of 200 kWh/t.

The unbeaten fibers of Eucalyptus and NBSK were additionally fractionated with various slot widths in order to narrow down the fiber length distribution. The fiber fractions used for sheet formation were designated by the mesh number used to obtain them (15, 50, 75, and 200 meshes/inch). Sheet grammage of unbeaten and unfractionated fibers were also varied, generating sheet densities of 30, 60, 75 and 90 g/m^2. In order to evaluate the impact of compression, NBSK and Eucalyptus pulp with a grammage of 90 g/m^2 were calendered between two steel rollers, which can be tempered at 120 °C. Contact pressures of 20, 40, 80, 160 and 320 N/mm were realized, while a feed rate of 0.5 m/min was consistently used.

2.2. Generating Hydrophilic Channels by Wax Printing

Hydrophilic microfluidic channels were generated by means of wax printing parallel rectangles with a 1, 2, 3, 4 or 5 mm gap along the length of the porous medium using a Xerox ColorQube 8580 printer (*Xerox Holding Corporation, Norwalk, USA*). Penetration of the wax into the substrate was then achieved by melting it in an oven at 125 °C for 20 s. This method to generate hydrophobic barriers in paper is literature known and well described in various publications. [17–19] If not explicitly stated otherwise, the hydrophilic channel width in the following experiments is 5 mm.

2.3. Spinning Device

The method to obtain characteristic pore radii along with a substrate coefficient for various porous media was described by us earlier. [16] In brief, a sample, into which a fluid can enter by capillary driven transport, is rotated to create a centrifugal force that counteracts the capillary force. Thereby, the dynamic process of imbibition is turned into a static one (Figure 1).

At the outer end of the rotating disc, an unlimited fluid reservoir is located. Any porous or capillary-active substrate can be connected to it and aligned towards the pivot point. The capillary driven force F_{Cap} directs towards the center, i.e. the rotation axis, while the centrifugal force F_{Cen} opposes it. Hence, the following force balance can be written:

$$F_{Cap} - \Delta F_{friction} = F_{Cen} \tag{2}$$

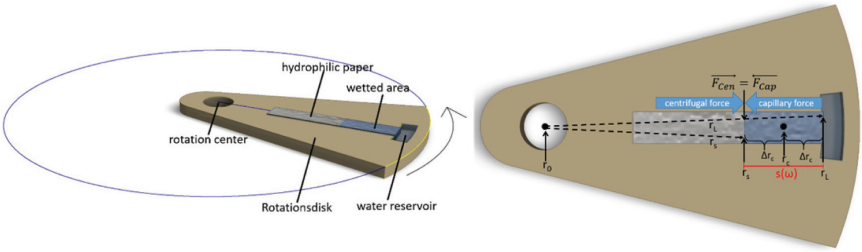

Figure 1. Schematic illustration of the rotating chuck, which contains a water reservoir at the outer end. On the chuck, a paper strip is mounted and wetted by the reservoir upon rotation.

Based on the friction $\Delta F_{friction}$ and centrifugal force, the fluidic slows down until it stops and a force equilibrium is established. Consequently, any fluid transport stops at this point, so that the equation simplifies to:

$$F_{Cap} = F_{Cen} \tag{3}$$

Expressing the wetting distance s(ω) at force equilibrium against angular velocity ω then yields:

$$s(\omega) = r_L - \sqrt{r_L^{\,2} - \frac{1}{\omega^2}\frac{4\gamma\cos(\theta)}{\rho\, r_{cap}}} \tag{4}$$

The equation shows that the wetting distance depends on the distance between the rotation center and the water reservoir (r_L), the surface tension of the fluid (γ), the contact angle (θ) and the fluid density (ρ).

We have, however, noticed that Equation 4 is not able to describe measured data of the wetting distance in dependance of angular velocity. Rather, the latter is always overestimated, which leads to Equation 4 being shifted towards higher values of angular velocity compared to the experimentally observed values. The reasons for this shift will be discussed later and will be addressed in more detail in future work. It should only be mentioned here that another force obviously counteracts the capillary force, so that a lower centrifugal force is sufficient to stop the imbibition. To account for this, we add a parameter to Eqution. 4, which in the following we refer to as the substrate coefficient α:

$$\omega_R = \omega + \alpha \tag{5}$$

The final equation then has the form:

$$s(\omega) = L\sqrt{L^2 - \frac{1}{(\omega+\alpha)^2}\frac{4\gamma\cos(\theta)}{\rho r_{cap}}} \tag{6}$$

For an experimental error estimation, 11 different rotational speeds were approached, the dynamic behavior was observed and the wetted distance at force equilibrium was plotted against the angular velocity:

At first, a rapid decrease in the rotational speed causes a rapid acceleration of the imbibition speed. But then, quickly, propagation slows down and comes to a standstill. The wetting distances at these force equilibria are then plotted against

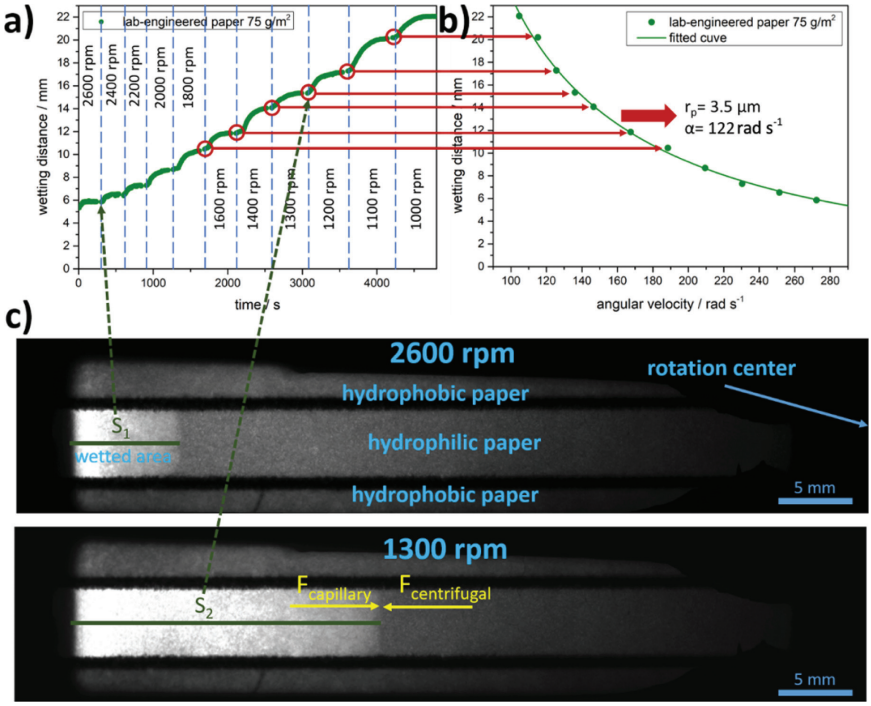

Figure 2. Application of the method on lab engineered Eucalyptus paper with a grammage of 75 g/m^2. (a) The wetting distance of the substrate is plotted against time at different rotation speeds. (b) The wetting distance at force equilibrium is taken from these measurements and is plotted against the angular velocity. A fit of the data to equation 6 then yields a median pore radius r_p and the pressure drop related substrate α coefficient. (c) Two images of the partly wetted paper at two different rotation speeds are shown.

the respective angular velocity. Then, a fit of this data to equation 6 yields a median pore radius r_p and the substrate α coefficient (Fig. 2). The dependence of wetting distance on angular velocity is also illustrated by two images, showing the fluid distance for two different rotational speeds at force equilibrium (Fig. 2c). In these images, wetted areas within the hydrophilic paper channel can clearly be distinguished from dry ones via the higher reflectivity of light.

2.3 Experimental Design of the Spinning Disc

To obtain strong mechanical properties at low weight, the spinning disc is made of acrylonitrile butadiene styrene (ABS) using a 3D printer (Raise 3D N2, *Irvine California USA*), which allows to create a design with numerous hollow structures (Figure 3).

The design includes water basins at the outer edges of the rotating chuck, which are filled upon rotation via a pipe system from water reservoirs within the chuck. In that moment, the paper strip gets in contact with water and imbibition towards

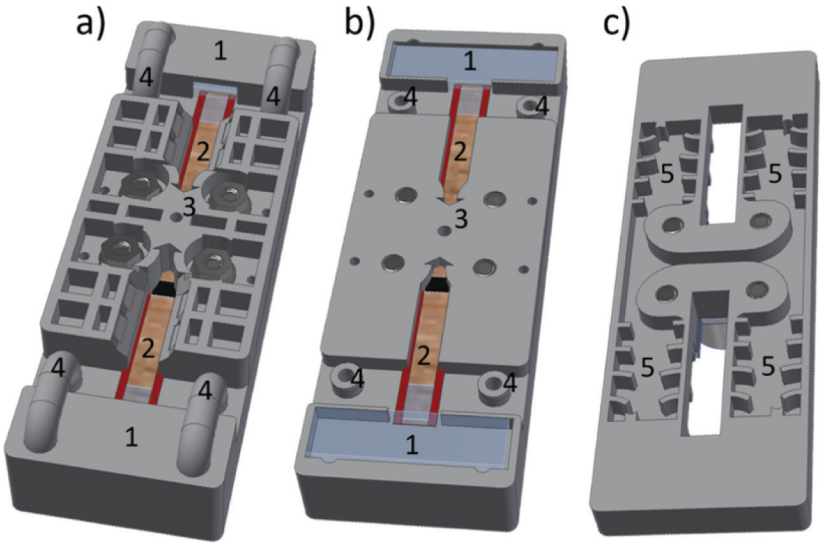

Figure 3. 3D renderings of the symmetrically constructed rotating chuck. (A) Top view of the assembled chuck. (B) Bottom part. (C) Top part. Water basins, placed at the outer edges (1), are filled via a pipe system (4) from water reservoirs (5) when the rotation starts. In that moment the hydrophilic paper strips (2) get in contact with the water and capillary driven fluid flow towards the center can take place. The papers are physically clamped by a top-lid placed on a bottom-chuck component preventing any movement of the substrate.

the center starts. The design allows the hydrophilic channel of the paper strip to be investigated by transmitted or reflected light from an LED, in order to distinguish already wetted from still dry areas. As the paper strip is clamped within the chuck only at the wax barriers, the hydrophilic paper channel only has contact to air during imbibition. Finally, the water reservoirs can be refilled during rotation to always ensure an infinite supply during experiments.

3. RESULTS AND DISCUSSIONS

Within the scope of this paper, the influence of the following intrinsic and extrinsic parameters of paper-based microfluidic devices were analyzed with respect to pore radius r_p and the substrate coefficient α in lab-engineered paper: Pulp type, freeness, fiber fraction, grammage, compression, and width of the microfluidic channel

3.1 Varying Pulp Type and Grammage

We first turned our focus on the investigation of different types of bleached pulp. For this, lab-made paper sheets were prepared from Eucalyptus, linters and NBSK pulp, respectively. The used fiber types differ in fiber length and morphology, and a detailed comparison of individual fiber properties is outlined in Table 1. The fiber anlaysis with respect to their fiber length, coarseness, curl and degree of fibrillation was examined and evaluated by means of a Fiber Image Analyzer FS5 (*Valmet AG, Espoo, Finnland*). The Shopper-Riegler value in order to determine the drainability of the pulp was obtained according to ISO 5267-1:1999

In brief, Cotton Linters consists of highly fibrillated and flexible fibers. Unbeaten Eucalyptus and NBSK fibers are smoother but differ significantly in geometric dimension (length/width). Softwood pulp consist of naturally longer and wider fibers than hardwood pulp. After preparation of handsheets with different grammages, paper stripes of defined length and width were cut and

Table 1. Tabular overview of fiber-specific characteristics

Pulp	*Shopper-Riegler* [SR]	*Mean fiber length* [mm]	*Mean fiber width* [μm]	*Coarseness* [mg/m]	*Fibrillation* [%]	*Curl* [%]
Eucalyptus	18.5	0.91	16.6	0.09	1.24	8.6
NBSK	14.1	2.08	27.2	0.24	1.04	10.9
Linters	18.0	1.44	25.3	0.21	1.84	15.5

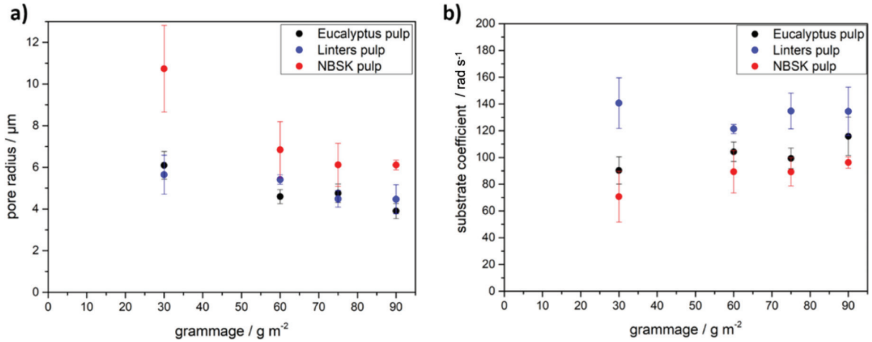

Figure 4. Paper materials made of Eucalyptus, cotton linters and NBSK pulp withs different grammages are analyzed with respect to the (a) characteristic pore radius and (b) the substrate coefficient.

porosity centrifuge measurements were carried-out, as explained in the experimental section above. Results of the pore-radius and the substrate coefficient as a function of the paper grammage are shown in Figure 4.

Regarding the dependency of the pore radius on the fiber type, it is evident that no significant change can be observed between Eucalyptus and linters pulps, while for NBSK papers the differences with respect to the characteristic pore radius and error bars are much greater. This could be due to the significantly larger and wider fibers along with the high coarseness values (fiber mass per length) of the softwood fibers which prevents a collapse of the fiber structure and forms an open network. Although Linters fibers are longer than Eucalyptus (Table 1), pore radii do not differ much due to the flexibility of Linters fibers.

By varying paper grammage, a decreasing pore radius is observed (Figure 4a), which can be attributed to the non-linear compression during the paper making process. Conversely, smaller pores go along with an increase of pressure drop, thus a slight increase in the substrate coefficient is measured at higher grammage (Figure 4b). A possible reason for this could be a difference in the morphology of the respective paper, in particular small fibrils at the surface of the fibers may influence the pressure drop significantly. Due to the refining process, the cotton Linters fibers have a much higher degree of fibrillation than the wood pulps. In order to investigate this hypothesis, we analyzed the paper morphologies by SEM (Figure 5). As can be inferred from the SEM images, the paper samples show some distinct features and differences. Paper sheets prepared from Linters fibers exhibit a significant amount of smaller (micro)fibrils and larger fibers. Paper sheets made from Eucalyptus fibers do not have such amounts of fine structures but rather exhibit smooth macro-fiber surfaces. Note that, although not visible in the SEM images

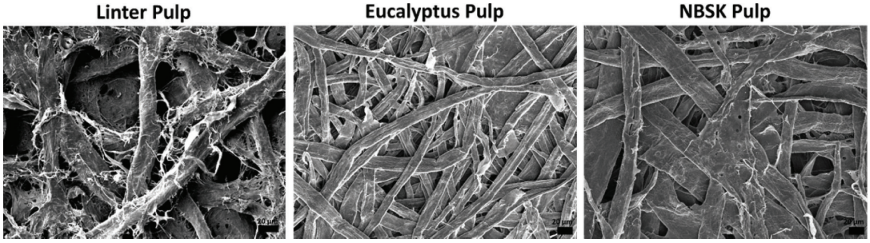

Figure 5. SEM-images of papers made of different pulps: cotton linters, Eucalyptus and NBSK.

Table 2. Overview of the median pore radius and substrate coefficient of Eucalyptus pulp when using water or 1,2-propanediol as the liquid

Fluid	*Pore radius* r_p / µm	*Substrate Coefficient* α / rad s^{-1}
Water	4.5 ± 0.1	103 ± 3
1,2-Propandiol	4.9 ± 0.2	122 ± 5

due to the necessary conditions during the imaging process (dry state, high vacuum), in contact with water, microfibrils do swell considerably at the surface of the macro-fiber, which will affect the interaction with the water molecules present in the macro-pores and within the swollen fibers, respectively. As both paper sheets have similar pore geometries, the differences in the substrate coefficient as shown before, may be attributed to the presence of larger friction forces due to the microfibrils present with Linters fibers. However, as can be seen from both the images and Table 1, NBSK has the least amount of fibrillation with much wider fibers, generating wider pores along with low substrate coefficients. Also, different fiber geometries can be seen on the SEM images, which are rather flat for NBSK, while Linters fibers are more rounded, as described in the literature. [20]

In order to evaluate swelling effects, another wetting liquid was used in addition to water to check the results using Eucalyptus pulp as an example. The liquid used was 1-2-propanediol (Table 2).

A comparison of the pore radii shows that smaller pores are obtained with water than with 1,2-propanediol, which could be due to swelling effects that are stronger in the presence of water. Higher values are also obtained for the substrate coefficient for the organic liquid despite the larger pores, which would reduce the pressure drop. But as 1,2-propanediol also has a much higher viscosity (42 mPa s), internal friction, which has an impact on the substrate coefficient, leads to higher values.

3.2 Varying Milling Degree

Next, we were interested in learning more about the influence of the fiber and paper sheet morphology on the pressure drop. For that, pulps were grounded with different mechanical energy inputs. Since no chemicals were used, it can be assumed that the chemical structure remains the same after this treatment. We used NBSK and Eucalyptus pulp and the fibers were treated with a lab-refiner as outlined in the experimental section at varying energy per mass of fibers. After the refining process, paper sheets were again formed by the Rapid Koethen technique and the fiber and sheet morphology was investigated by SEM analysis. Figure 6 shows examples of SEM images taken from the lab-made sheets. As shown in the figure, the fibrillation of the fibers increases with increasing refining energy, and fibrillation can lead to an increase in fuzzy, amorphous fiber interface fractions. The latter may result in an enhanced degree of swelling of the fibers in contact with water. Note that the process also slightly shortens the fibers (Table 3).

After finding a higher amount of highly water swellable fibrils in dependence of beating energy, we next investigated how this change in fiber and sheet morphology will affect the analysis with the porosity centrifuge. Figure 7 shows the results of this analysis, where the pore radius and the substrate coefficient are now plotted as a function of the refining energy ("milling power"). It can be seen that, with increasing milling power, the pore radius decreases from about 5 μm (Eucalyptus) / 6 μm (NBSK) in the unrefined state (i.e. zero milling power) to about 3 μm / 4.5 μm for the strongly refined state (milling power: 200 kWh/t). As already seen above, NBSK pulp again generates larger pores due to its significant lager fibers along with higher coarseness values. The decrease in pore radius corresponds to a relative decrease of about 20–30% and can be attributed to more compact paper sheets and pore geometries with slightly shorter fibers, higher flexibility in the fiber structure and a higher degree of swelling of the sheets through the decrystallization processes during the milling process. The substrate

Table 3. Influence of refining milling power on Eucalyptus fiber characteristics

Milling power [kWh/t]	*Mean fiber length* [mm]	*Fines* [%]	*Fibrillation* [%]
0	0.91	14.6	1.2
15	0.91	14.8	1.2
50	0.90	15.6	1.2
100	0.89	16.0	1.3
150	0.87	16.35	1.3
200	0.85	17.6	1.4

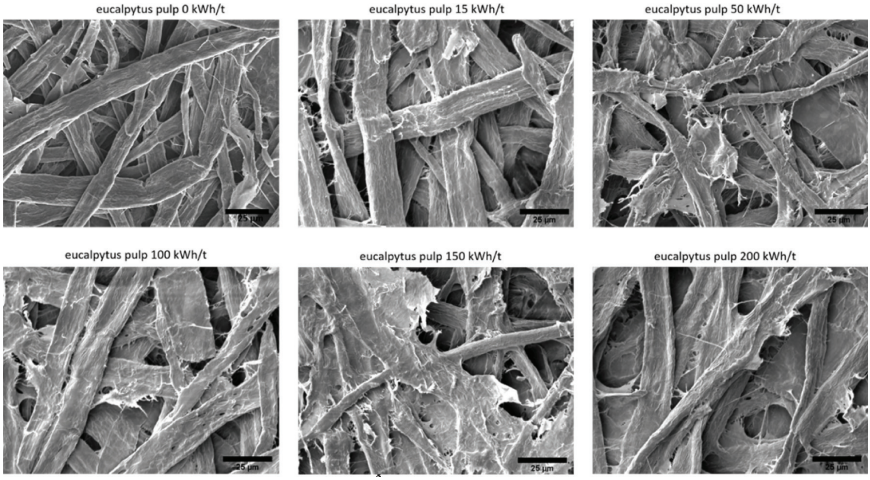

Figure 6. SEM-images for papers (75 g/m^2) made of Eucalyptus pulp but beaten with different energy: 0, 15, 50, 100, 150 and 200 kWh/t.

coefficient shows a strong increase from about 100 (for both pulps) in the unrefined state to 167 (NBSK) / 255 (Eucalyptus) for the strongly refined state (milling power: 200 kWh/t).

Both, the decrease in the pore radius as well as the increase in the substrate coefficient have a direct link to the changes in the morphology of the fibers and the paper sheets due to fiber refinements. The increase of the substrate coefficient

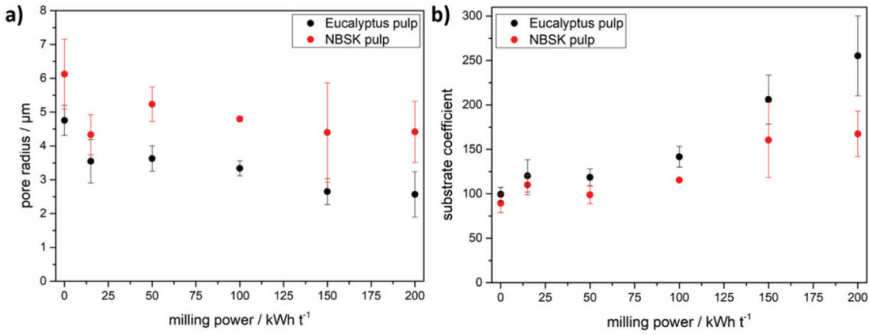

Figure 7. Plotting experimental characteristic pore radius (a) or substrate coefficient (b) against the milling power for papers made out of Eucalyptus or NBSK pulp with a grammage of 75g/m^2.

may be attributed not only to the slight decrease in pore radius but also to changes in morphology. The fine structural elements on the fiber surfaces provide more contact between the fibers and thereby a denser paper structure. At the same time, the rougher fiber surfaces and higher degree of swelling of this interphase also increases friction during fluid dynamics, which may be reflected in the increasing substrate coefficient.

3.3 Fractionation of Fibers

So far, we have not focused on the impact of changes in the fiber geometry, such as length (and width) on the outcome of the analysis by our method. However, as in particular fiber length can impact the pore structure of the sheet, changes to this parameter should also be detectable with it. Eucalyptus and NBSK fibers were fractionated for length as outlined in Table 4. Of note, this process also sorts out fine fibrils (fines) from the macro-fiber fraction. Fiber fractions were then used to form paper sheets as outlined above.

The results show that for both fiber types, longer fibers yield lager pores (Figure 8, left). Interestingly, if the fiber lengths are similar for both fiber types (fiber length about 0.6 mm), so are the resulting pore radii. However, with increasing fiber length, the pore radius of Eucalyptus paper increases much faster compared to NBSK. Although we do not have an exact proof for this, one may argue that more flexible softwood fibers can arrange in a more densely packed sheet than the stiffer hardwood fibers. As such, relative increase of the pore radius for softwood paper sheets with increasing fiber length is less pronounced. Such differences between hard- and softwood fibers have been reported elsewhere, yet not with identical fiber types. [21]

In Figure 8 (right) the substrate coefficient is plotted as a function of the fiber length. As is shown, the substrate coefficient of the different fiber types at varying

Table 4. Mean fiber characteristics at different fiber fraction for Eucalyptus and NBSK pulp

(n.d. – not determined)

Fiber fraction meshes/inch	*Eucalyptus*			*NBSK*		
	Fiber length / mm	*Fiber width / μm*	*Curl / %*	*Fiber length / mm*	*Fiber width / μm*	*Curl / %*
14	n.d.	n.d.	n.d.	2.2	29.0	10.0
30	0.9	16.8	9.6	1.6	27.1	10.0
50	0.8	16.5	7.7	1.1	25.4	9.7
200	0.6	16.6	6.3	0.6	22.6	8.0

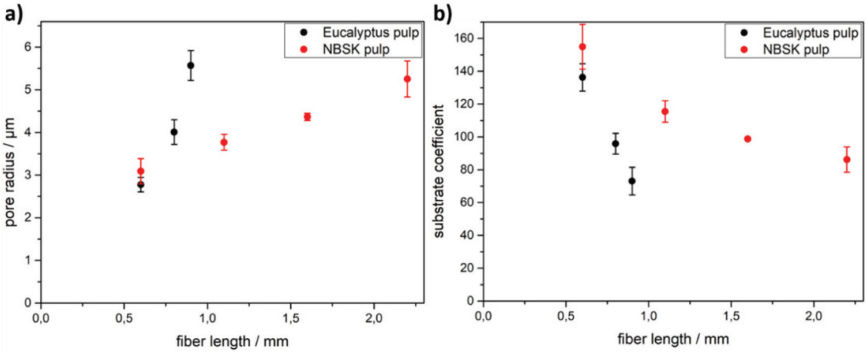

Figure 8. Influence of fiber length on the pore radius (a) and the substrate coefficient (b) for papers (75 g/m^2) made of Eucalyptus and NBSK pulp.

fiber length shows an inverse behavior as compared to the pore radius, respectively. With increasing fiber length, we do observe a much stronger decrease of the coefficient with Eucalyptus fibers compared to NBSK. The latter may be explained by both, geometric structure of the porous sheet (Figure 8, left) as well as considering the morphology of the fibers. With respect to the latter, higher fractions of amorphous regions in NBSK lead to a higher degree of swelling and thus can result in higher friction forces during capillary imbibition. The latter may therefore result in lower pressure drop and thereby cause a larger substrate coefficient at comparable pore radii.

3.4 Influence of Channel Width

A next question relates to the design of the paper stripes that can be measured within our device, and if the width of the paper strip matters and interferes with our analysis. The influence of channel width on fluid dynamics with paper based fluidic devices in non-rotational transport measurements has been described in literature. [12, 22] A reduction in fluid transport speed is observed when a hydrophobic boundary narrows the hydrophilic parts. Interestingly, this reduction occurs as soon as the channel width is smaller than a typical fiber length of the pulp being used in the studies. [8] In order to investigate whether the channel width affects the outcome of the analysis of the pore radius and the substrate coefficient, we first prepared small hydrophilic paper strips. As it was not trivial to mount narrow paper strips into our device, we modelled the hydrophobic (air) boundaries by wax-printed barriers. Thin wax stripes are printed on our lab-made paper sheets and by heating imbibe into the open pore structure of the paper. By

this technique thin areas down to channel widths of 1.5 mm were designed, which approaches the length of single fibers. Figure 9 shows images of the so prepared samples as they are investigated in our rotation device. Results are shown in Figure 10, where the pore radii and the substrate coefficients are plotted as a function of channel width.

If the channel width is larger than 1 mm, all measured pore sizes remain at about 3.5 μm to 4 μm, for Eucalyptus and NBSK, regardless of the channel width. With smaller channels, however, we observe an increase in standard deviation that yet is not trivial to explain. However, the findings are in line with an earlier

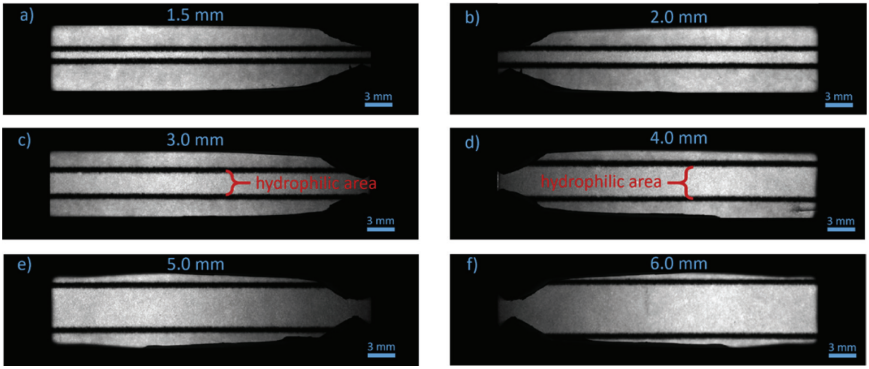

Figure 9. Images of paper strips with different hydrophilic channel widths mounted in the porosity centrifuge. (a) 1.5 mm, (b) 2.0 mm, (c) 3.0 mm, (d) 4.0 mm, (e) 5.0 mm and (f) 6.0 mm.

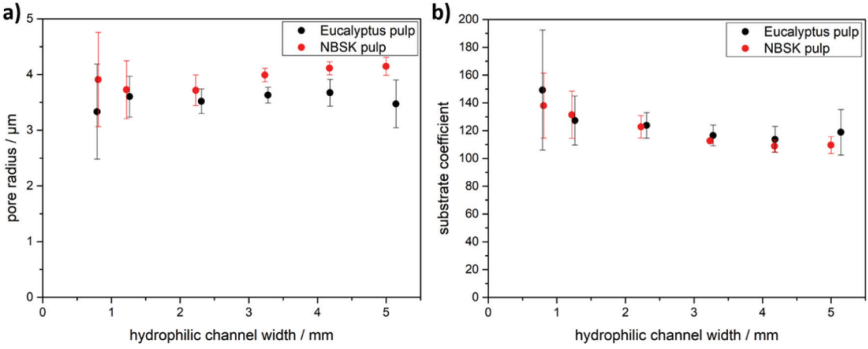

Figure 10. Influence of channel with on a) the median pore radius and b) the substrate coefficient for papers made of Eucalyptus or NBSK pulp.

work of our group, where it was reported that fluid transport rates in paper microfluidic channels are not significantly affected by channel width as long as this value stays above the geometric fiber length. [8]

3.5 Cold/hot Calendaring

Significant changes to the pore radii within a paper material without changing fiber morphology or chemical modification is possible through e.g. mechanical compression. The degree of paper compression can be varied by applying different forces to the two iron rollers between which the paper sheet is placed. Furthermore, the rolls can be used cold (room temperature) or heated (120 °C), which can lead to different amounts of compression due to additional drying effects. To evaluate the effect of compressive force on pore structure in the wetted state, five

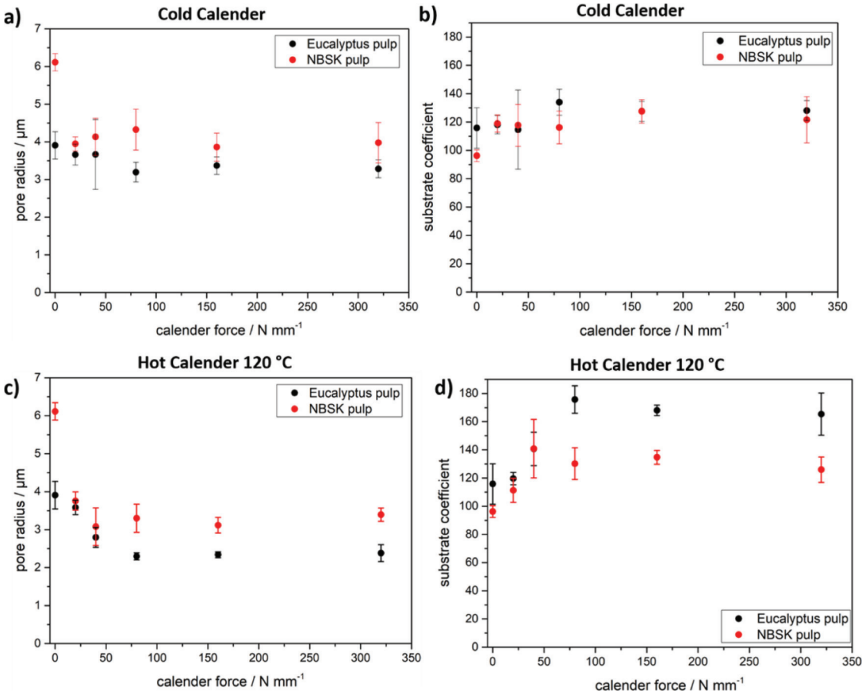

Figure 11. Analyzing the impact of compressed paper made of Eucalyptus or NBSK pulp in respect of pore radius for (a) cold or (c) hot calendring along with the substrate coefficient as well for (b) cold and (d) hot rollers.

different laboratory sheets of Eucalyptus and NBSK pulp were applied. Figure 11 shows the analysis of centrifuge porosity measurements (i.e. pore radius and substrate coefficient) as a function of the applied force. Note that we do plot the force applied by one of the two iron rollers.

When NBSK papers have been calandered at low temperature, a significant reduction in pore radius can be observed in comparison to non-calendered samples. The reduction, however, levels of at a pore radius of about 4 μm already at forces larger than 25 N/mm and stays constant even at very large forces of more than 300 N/mm. A similar trend is observed for the substrate coefficient that more or less is not affected by the calander-treatment. At higher temperatures, however, such hot calandering treatment leads to a more pronounced decrease in pore radius and a more visible increase in the substrate coefficient as a function of the calandering force, respectively. Differences between the different pulps used in this experiment series are visible however, rather marginal despite the fact that non-calandered NBSK pore radius is much larger than the pore radius of non-treated eucalyptus sheets. Although we do not fully understand this behavior yet, one may again argue with different fiber flexibility and fiber length of the different pulp as discussed before.

4. CONCLUSION

In this paper, we introduce a new time efficient and simple to elaborate laboratory method, to characterize the porous structure of paper in contact with a swelling solvent (i.e. water). Using centrifugal forces that counter-balance capillary forces during imbibition of paper sheets with water as the solvent, we are able to analyze the characteristic pore size of paper in a rapid and reproducible manner. Moreover, the method provides easy access to investigate the effect of fiber type, fiber length, fines content, fiber beating and post-calandering on pore sizes, due to the sensitivity of the method. We also show that the width of the substrate used does not influence the measurements. Last but not least it should be noted that the introduced method is not limited to water as a solvent but can in principle be used with almost any solvent that shows capillary driven fluid imbibition.

Finally, besides the characteristic pore radius, the method also introduces a parameter α, the substrate coefficient. We are well aware that in the present work, the parameter is not yet sufficiently specified, i.e. what physical nature it is and from which individual quantities it is composed and derived. What we can state for sure, however, is that the relationship between capillary migration distance and angular velocity – derived from the equilibrium of forces – can only be fitted to the measured data by using this parameter and that the equation thus modified describes the data exceptionally well. Furthermore, we can state that alpha

increases with the roughness and/or porosity of the substrate. For exactly this reason, we have termed it a "substrate coefficient". To get to the bottom of the nature of this parameter, we will next perform a more detailed mathematical modeling and numerical simulations of our experiments. However, samples with complex porosity such as paper sheets pose a hurdle here, as they are extremely difficult or even impossible to simulate to date. We will therefore further address this topic to gain a better understanding of this substrate coefficient via measurements on more simple capillaries (e.g. glass-capillaries, etc.) with different diameters, which can be modeled more easily. Outcome of these experimental as well as simulation studies will be reported in future communications.

FUNDING SOURCES

Funded by the Deutsche Forschungsgemeinschaft (DFG) within the Collaborative Research Center 1194 "Interaction of Transport a Wetting Processes" – Project ID 265191195.

NOTES

The authors declare no competing financial interest.

ACKNOWLEDGMENT

We thank Sören Postulka and Maximilian Nau for valuable technical help and discussion.

REFERENCES

1. Rouquerol, J., G. Baron, R. Denoyel, H. Giesche, J. Groen, P. Klobes, P. Levitz, A.V. Neimark, S. Rigby, R. Skudas, K. Sing, M. Thommes, and K. Unger, Liquid Intrusion and Alternative Methods for the Characterization of Macroporous Materials (IUPAC Technical Report). *Pure and Applied Chemistry*, 2011. 84(1): pp. 107–136.
2. Lovikka, V.A., P. Khanjani, S. Väisänen, T. Vuorinen and T.C. Maloney, Porosity of Wood Pulp Fibers in the Wet and Highly Open Dry State. *Microporous and Mesoporous Materials*, 2016. 234: pp. 326–335.
3. Thommes, M., K. Kaneko, A.V. Neimark, J.P. Olivier, F. Rodriguez-Reinoso, J. Rouquerol and K.S.W. Sing, Physisorption of Gases, with Special Reference to the

Evaluation of Surface Area and Pore Size Distribution (IUPAC Technical Report). *Pure and Applied Chemistry*, 2015. 87(9–10): pp. 1051–1069.
4. Toussaint, R., B. Sandnes, D. Koehn, P. Szymczak and E. Aharonov, *Flow and Transformations in Porous Media*. 2017: Frontiers Research Topics.
5. Walji, N. and B. MacDonald, Influence of Geometry and Surrounding Conditions on Fluid Flow in Paper-Based Devices. *Micromachines*, 2016. 7(5).
6. Su, Y., G. Chen and Q. Yuan, Effect of Viscosity on the Hydrodynamics of Liquid Processes in Microchannels. *Chemical Engineering & Technology*, 2014. 37(3): pp. 427–434.
7. Fu, E., B. Lutz, P. Kauffman and P. Yager, Controlled Reagent Transport in Disposable 2D Paper Networks. *Lab Chip*, 2010. 10(7): pp. 918–920.
8. Böhm, A., F. Carstens, C. Trieb, S. Schabel and M. Biesalski, Engineering Microfluidic Papers: Effect of Fiber Source and Paper Sheet Properties on Capillary-driven Fluid Flow. *Microfluidics and Nanofluidics*, 2014. 16(5): pp. 789–799.
9. Chang, S., J. Seo, S. Hong, D.-G. Lee and W. Kim, Dynamics of Liquid Imbibition through Paper with Intra-fibre Pores. *Journal of Fluid Mechanics*, 2018. 845: pp. 36–50.
10. Washburn, E.W., The Dynamics of Capillary Flow. *Physical Review*, 1921. 17(3): pp. 273–283.
11. Mirzajanzadeh, M., V.S. Deshpande and N.A. Fleck, Water Rise in a Cellulose Foam: By Capillary or Diffusional Flow? *Journal of the Mechanics and Physics of Solids*, 2019. 124: pp. 206–219.
12. Hong, S. and W. Kim, Dynamics of Water Imbibition through Paper Channels with Wax Boundaries. *Microfluidics and Nanofluidics*, 2015. 19(4): pp. 845–853.
13. Chang, S. and W. Kim, *Dynamics of Water Imbibition through Paper with Swelling. Journal of Fluid Mechanics*, 2020. 892.
14. Böhm, A. and M. Biesalski, Paper-based Microfluidic Devices: A Complex Low-cost Material in High-tech Applications. *MRS Bulletin*, 2017. 42(05): pp. 356–364.
15. Masoodi, R. and K.M. Pillai, Darcy's Law-based Model for Wicking in Paper-like Swelling Porous Media. *AIChE Journal*, 2010: pp. NA–NA.
16. Postulka, N., T. Meckel and M. Biesalski, Porosity Centrifuge: Determination of Pore Sizes of Swellable Porous Materials under Hypergravity. *Langmuir*, 2021. 37(29): pp. 8746–8752.
17. Carrilho, E., A.W. Martinez and G.M. Whitesides, Understanding Wax Printing: A Simple Micropatterning Process for Paper-based Microfluidics. *Anal Chem*, 2009. 81(16): pp. 7091–7095.
18. Postulka, N., A. Striegel, M. Krausse, D. Mager, D. Spiehl, T. Meckel, M. Worgull and M. Biesalski, Combining Wax Printing with Hot Embossing for the Design of Geometrically Well-Defined Microfluidic Papers. *ACS Appl Mater Interfaces*, 2019. 11(4): pp. 4578–4587.
19. Qamar, A.Z., K. Amar, P. Kohli, F. Chowdhury and M.H. Shamsi, Wax Patterned Microwells for Stem Cell Fate Study. *RSC Advances*, 2016. 6(106): pp. 104919–104924.
20. Sczostak, A., Cotton Linters: An Alternative Cellulosic Raw Material. *Macromolecular Symposia*, 2009. 280(1): pp. 45–53.

21. Mayr, M., R. Eckhart, H. Winte and W. Bauer, A Novel Approach to Determining the Contribution of the Fiber and Fines Fraction to the Water Retention Value (WRV) of Chemical and Mechanical Pulps. *Cellulose*, 2017. 24(7): pp. 3029–3036.
22. Castro, C., C. Rosillo and H. Tsutsui, Characterizing Effects of Humidity and Channel Size on Imbibition in Paper-based Microfluidic Channels. *Microfluidics and Nanofluidics*, 2017. 21(2).

POROSITY CENTRIFUGE: ANALYSIS OF THE POROUS STRUCTURE OF PAPER IN CONTACT WITH WATER UNDER HYPERGRAVITY CONDITIONS

Niels Postulka[1], *Michelle Seibert*[1], *Andreas Geißler*[1], *Mathis Fricke*[2], *Dieter Bothe*[2], *Tobias Meckel*[1] *and* *Markus Biesalski*[1]

[1] Macromolecular Chemistry and Paper Chemistry, Department of Chemistry, Technical University of Darmstadt, Alarich-Weiss-Str. 8, 64287 Darmstadt, Germany
[2] Mathematical Modelling and Analysis, Department of Mathematics, Technical University of Darmstadt, Alarich-Weiss-Str. 10, 64287 Darmstadt, Germany

Robert Pelton McMaster University

First, a comment that 7 or 8 years ago I attended a workshop in the US, all the big leaders in paper based lateral flow research were there. One of the things I learnt is that the biochemists love nitrocellulose because they bind antibodies very easily, I believe. But the people, who were actually from start-up companies that were trying to work in this area, said that there was a real problem with the nitrocellulose in batch to batch variation. I think there is a big opportunity for the cellulose community to do something better. I have a question: do you assume that for a given contact angle, the curvature of the air–water interface is constant? Or does it change as the flow slows down and stops?

Discussion

Markus Biesalski

We did some experiments in glass capillaries. I have to admit I did not put it in because it has a different configuration. With glass capillaries, you only need very little centrifugal force to push the water out. What we did is we actually filled a glass capillary, closed it on the bottom and we did the rotation and what you can do there is microscopically come to a meniscus that is completely flat, but you need 190 G force to do so.

Janet Preston Imerys Minerals Ltd

I was wondering if you could look at a paper coating with this technique, possibly applying the paper coating on a non-porous substrate so you did not have any fibre influence? Studying how the fluid passed through the coating would be interesting for studies of printing and various other uses such as barrier coatings.

Markus Biesalski

As long as we have technically enough contrast, it should be doable.

Janet Preston

Have you tried it or do you plan on trying it?

Markus Biesalski

We have not tried it yet.

Janet Preston

But you might?

Markus Biesalski

These are all uncoated paper. We just started, yet we will also look into other samples.

Johann Tryding Tetra Pak Packaging Solutions

I gave a question about the boundary conditions. Are they clamped or are they free?

Markus Biesalski

What we do is, we have this wax printed paper and at the boundaries, they are clamped. The inner part where we have the hydrophilic channel, it is totally free standing.

Johann Tryding

So, it is not what I was thinking. If it is clamped then is the clamping pressure a problem?

Markus Biesalski

No, we actually investigated this.

Gil Garnier Monash University

Can you please put on slide 12, the nice flow with the FITC-dye? First, this is beautiful work. What you have shown us, for me, is the best work we have seen of classical flow in paper. Now my question: if I look here, what I do not see is a flowing capillary, a slick and slip flow along fibres, so I have two questions. The Washburn equation, is it by luck that we see that the length varies with a square root of time such as with the first question? And second, what is the physical meaning of the radius in the paper, and here if you have radius of 4 micron, does it mean if I take a suspension of latex with 1 micron beads it will go, but one of 6 micron beads will not?

Markus Biesalski

That is a beautiful question. I will answer the last question first because these are exactly the experiments that I was doing and right now doing, but we like to learn about really what we call here characteristic or apparent radius, what kind of radius we are talking about. I cannot say it's the median or so, I would not dare to, but this is something that we definitely do, thank you. Maybe shortly a remark to this video here. Actually, it is only here at the front where we see the peak in the fluorescence and as soon as the fluorescence equals here 0.5 and you can, if you look very carefully, see a shade right behind the high fluorescence part. This shade is the capillary filling. At the end of the video, if it's all the way over to the right-hand side, as it is completely filled with water, even if it is hard to see it. Maybe we should transfer this to the very end of the session where we may have a general discussion about whether Lucas-Washburn should be discussed.

Discussion

Lars Wågberg KTH Fibre and Polymer Technology

I felt you were using a circular argument in the beginning when you used the Lucas-Washburn equations to calculate the pore radii in the papers. So, when you calculate the radius using Lucas-Washburn, you said you arrived at a 4 micrometre radius. Then you made a 4 micrometre paper which turned out to be 8 micrometre? Can you please explain?

Markus Biesalski

How did I do the 4 micrometre radius?

Lars Wågberg

It sounds like a circular argument. How do you determine the radii?

Markus Biesalski

Well, of course we did it the other way around. We first measured the 4 micrometre radius and then we said okay, now let's measure what we should get out by Lucas-Washburn.

Lars Wågberg

But how did you get the different curves in your diagram?

Markus Biesalski

The one curve is not data. This is just fit. So this is just a drawn line with a slope of 11.8, no data. The data is shown here as dots and this is real data with just linear fit without putting in the exact values. If we put in the exact values, we end up with a blue line. That is the difference.